Bimodal Loop−Loop Interactions Increase the Affinity of RNA Aptamers for HIV-1 RNA Structures†

David Boucard, Jean-Jacques Toulmé, and Carmelo Di Primo*

Université Victor Segalen, Bordeaux, F-33076, France, INSERM U386, Bordeaux, F-33076, France, and Institut Européen de Chimie et Biologie, Pessac, F-33607, France

Received June 21, 2005; Revised Manuscript Received August 29, 2005

ABSTRACT: Multiple loop−loop interactions between adjacent RNA hairpins regulate gene expression in different organisms. To demonstrate that such natural interactions could be mimicked for generating RNA ligands that are able to recognize simultaneously at least two structured RNA targets, a double kissing complex model was designed. The target consisted of two HIV-1 transactivating responsive (TAR) RNA variants, BRU and MAL, connected by a non-nucleotidic linker. The double ligand was generated by combining the corresponding hairpin aptamers, R06BRU and R06MAL, identified previously by in vitro selection [Ducongé, F., and Toulmé, J. J (1999) *RNA 5*, 1605−1614]. The resulting interaction was analyzed by thermal denaturation monitored by UV spectroscopy, electrophoretic mobility shift assays (EMSAs), and surface plasmon resonance (SPR) experiments. The bimodal complex was characterized by a binding equilibrium constant increased by at least 1 order of magnitude compared to that of the complexes between the individual parent hairpins. This resulted from a slower dissociation rate. We then made use of such a strategy for targeting two structured functional motifs of the folded 5′ untranslated region (5′UTR) of HIV-1. Two bivalent RNA ligands were designed that targeted simultaneously the TAR and dimerization initiation site (DIS) hairpins or the TAR and poly(A) ones. The results show that these ligands also displayed enhanced affinity for their target compared to the individual molecules. The work reported here suggests that bimodal structured RNA ligands might provide a way of increasing the affinity of aptamers for folded RNA targets.

RNA kissing complexes are functional motifs formed between stem−loop structures. Such motifs are involved in the regulation of several biological processes in both prokaryotic and eukaryotic organisms (*1*). Some natural processes make use of multiple loop−loop interactions between adjacent hairpins. In *Escherichia coli*, the ColE1 plasmid replication is controlled by two RNA transcripts, RNA I and RNA II, that fold as three adjacent hairpins (*2*−*4*). The interaction between these two RNAs is initiated with base pairing of at least two complementary loops. This transient kissing complex is stabilized by the structure-specific plasmid-encoded protein Rop. The complex between the two RNAs subsequently "zips up" to form an extended RNA duplex. mRNA translation in *E. coli* can also be regulated through multiple loop−loop interactions. OxyS is a small untranslated RNA induced in response to oxidative stress that represses the expression of several genes (*5*). The secondary structure of OxyS RNA shows three stem−loop structures. Two of them are engaged in loop−loop interactions with the two nonadjacent stem−loop structures of the *fhla* mRNA (*6*−*8*). Such a double kissing complex prevents the ribosomes from binding to the Shine Dalgarno sequence repressing the translation of the transcriptional activator encoded by the *fhla* gene.

We endeavored to mimic these multiple interactions by designing RNA ligands able to bind simultaneously to two stem−loop structures of an RNA target. Compared to the targeting of a single structure, the proposed strategy is expected to increase the affinity and the specificity of such ligands for their target.

This work focused first on the analysis of a model of interaction consisting of a double kissing complex derived from the individual loop−loop complex identified previously by in vitro selection against the transactivation responsive (TAR)[1] element of the human immunodeficiency virus type 1 (HIV-1) (*9*). The TAR imperfect hairpin is a 57-nucleotide RNA with a 6-nucleotide apical loop. TAR displays a bulge in the upper part of the hairpin, which constitutes part of the binding site of the viral protein Tat (*10*, *11*). Hairpins corresponding to the top part of the two TAR variants, BRU and MAL, which differ by a single residue in the loop were connected by a non-nucleotidic linker to generate the bivalent target. The corresponding specific BRU and MAL aptamers, identified previously by in vitro selection against TAR (*9*), were connected similarly to generate the bivalent ligand. Electrophoretic mobility shift assays (EMSAs) and surface plasmon resonance (SPR) experiments showed that the double kissing complex is characterized by a binding

† D.B. is the recipient of a FRM/CNRS/Région Aquitaine fellowship. This work is supported in part by the Sidaction and the ANRS.

* To whom correspondence should be addressed: Institut Européen de Chimie et Biologie, 2 rue Escarpit, 33607 Pessac cedex, France. Telephone: 33 (0)5 40 00 30 50. Fax: 33 (0)5 40 00 30 04. E-mail: c.diprimo@iecb.u-bordeaux.fr.

[1] Abbreviations: HIV-1, human immunodeficiency virus type 1; TAR, transactivation responsive element; 5′UTR, 5′ untranslated region; PBS, primer binding site; DIS, dimerization initiation site; EMSA, electrophoretic mobility shift assay; SPR, surface plasmon resonance; RU, resonance unit(s); TOP, tethered oligonucleotide probe; RRE, Rev response element.

10.1021/bi051187f CCC: $33.50
Published on Web 01/12/2006

equilibrium constant increased by at least 1 order of magnitude compared to that of the individual parent loop−loop complexes. This enhanced stability originates in a slower dissociation rate.

We then tried to design bivalent RNA ligands able to interact simultaneously with two stem−loop structures of the 5′ untranslated region (5′UTR) of the HIV-1 BRU genome. Two adjacent hairpins were used to target simultaneously the TAR and dimerization initiation site (DIS) hairpins. A ligand consisting of a hairpin connected to a linear oligonucleotide was generated to bind the TAR and poly(A) hairpins. Complexes formed between the 5′UTR and bivalent RNA ligands exhibit enhanced stability compared to those formed with single ligands. Therefore, compared to monovalent ligands, bifunctional RNA molecules provide a way of increasing the affinity for folded RNA targets.

MATERIALS AND METHODS

Oligonucleotides. All RNA molecules except the HIV-1 BRU 5′UTR were either synthesized on an Expedite 8908 synthesizer or purchased from Dharmacon Research Inc. and purified by electrophoresis on denaturing polyacrylamide gels.

PCR Amplification and T7 Transcription. The HIV-1 BRU 5′UTR molecule was synthesized by in vitro transcription of DNA fragments obtained by PCR amplification during which a T7 promoter sequence was introduced thanks to a sense primer. The Bluescript-5′LTR plasmid was used as a template for PCR amplification with the T7-2 sense primer 5′-AAT TCT AAT ACG ACT CAC TAT AGG GTC TCT CTG GTT AGA CCA G (the underlined portion corresponds to the promoter region) and the R-290 antisense primer (5′-CCA GTC GCC TCC CCT CGC CTC TTG). DNA fragments containing the T7 promoter sequence and the TAR, poly(A), PBS, and DIS elements of the HIV-1 BRU 5′UTR were obtained. The DNA products were purified with the Nucleospin kit (Macherey-Nagel) and then transcribed for 6 h at 37 °C, using the AmpliScribe T7 transcription kit (Tebu). The transcripts were purified on a denaturing 8% polyacrylamide−7 M urea gel. The pure samples were ethanol precipitated, desalted by being washed with 70% ethanol, resuspended in water, and stored at −20 °C.

UV-Monitored Melting Experiments. Thermal denaturation of RNA−RNA complexes (1 μM each oligonucleotide) in 20 mM sodium cacodylate buffer (pH 7.3) at 20 °C, containing 140 mM potassium chloride, 20 mM sodium chloride, and 1 mM magnesium chloride, was monitored with a Uvikon XL spectrophotometer (Bio-Tek Instruments). Denaturation of the samples was carried out by increasing the temperature at a rate of 0.4 °C/min from 4 to 85 °C and was followed at 260 nm. The absorption at 310 nm was used as a reference. Prior to the experiments, single RNA hairpins were heated at 90 °C for 1 min, put on ice for 5 min, and allowed to warm at room temperature. Double hairpins were heated at 65 °C for 5 min and then cooled at room temperature to prevent alternative foldings. RNA samples were then mixed at room temperature and allowed to interact 15 min before cooling to 4 °C. The experiment started after 45 min at this temperature. The melting temperature, T_m, was given as the maximum of the first derivative of the UV melting curve.

Electrophoretic Mobility Shift Assay. The apparent dissociation equilibrium constants, K_d, of the complexes were determined using 4000 cpm per lane of 5′-end-labeled [γ-^{32}P]-RNA incubated with an increasing concentration of ligand for at least 3 h at room temperature in 20 mM HEPES buffer (pH 7.3) at 20 °C, containing 20 mM sodium acetate, 140 mM potassium acetate, and 1 mM magnesium acetate. Each mixture was loaded onto nondenaturing gels [10% acrylamide/bisacrylamide at a 19:1 ratio in 50 mM Tris-acetate (pH 7.3) at 20 °C, and 1 mM magnesium acetate] equilibrated at 4 °C. The electrophoresis was carried out at 200 or 150 V, at 4 °C, for 12 h. The radioactivity was quantitated with an Instant Imager apparatus (Hewlett-Packard). The K_d was deduced from data-point fitting of the titration curves using Kaleidagraph 3.0 (Abelbeck software) according to eq 1:

$$[\mathrm{RNA}] = \{[\mathrm{RNA}]_0 + [\mathrm{Oligo}]_0 + K_d \pm \sqrt{([\mathrm{RNA}]_0 + [\mathrm{Oligo}]_0 + K_d)^2 - 4[\mathrm{RNA}]_0[\mathrm{Oligo}]_0}\}/\{2[\mathrm{RNA}]_0\} \quad (1)$$

where $[\mathrm{RNA}]_0$ and $[\mathrm{Oligo}]_0$ are the initial concentrations of the radiolabeled probe and the oligonucleotide ligand, respectively, and [RNA] is the concentration of the bound radiolabeled probe.

Surface Plasmon Resonance Kinetic Measurements. SPR experiments were performed on a BIAcore 2000 apparatus (Biacore AB, Uppsala, Sweden) running with the BIAcore 2.1 software. The biotinylated target RNA was immobilized on carboxymethylated dextran sensor chips (CM5, Biacore AB) coated with streptavidin according to the procedure described in the BIA Applications Handbook. Binding kinetics were determined at 23 °C in 20 mM HEPES buffer (pH 7.3) at 20 °C, containing 20 mM sodium acetate, 140 mM potassium acetate, and 1 mM magnesium acetate. All RNA samples were prepared in this buffer and injected at a rate of 20 μL/min.

Nonlinear regression analysis of a single sensorgram was used to determine the kinetic parameters of the complex formation. The data were analyzed with BIA-Evaluation 3.0. Two different models were used depending on the studied complex. The first was a simple reversible reaction mechanism:

$$\mathrm{A} + \mathrm{B} \underset{k_{off}}{\overset{k_{on}}{\rightleftharpoons}} \mathrm{AB}$$

where A and B stand for the immobilized biotinylated ligand and the injected RNA analyte in solution, respectively. The association and dissociation rate constants, k_{on} and k_{off}, respectively, were determined from direct curve fitting of the sensorgrams according to eqs 2 and 3 for the association and dissociation phases, respectively:

$$R = \frac{k_{on}CR}{k_{on}C + k_{off}} 1 - e^{-(k_{on}C + k_{off})(t - t_0)} \quad (2)$$

$$R = R_{t0} e^{-k_{off}(t - t_0)} \quad (3)$$

where R is the signal response, R_{max} the maximum response level, R_{t0} the response at the end of the injection, and C the molar concentration of the injected RNA molecule.

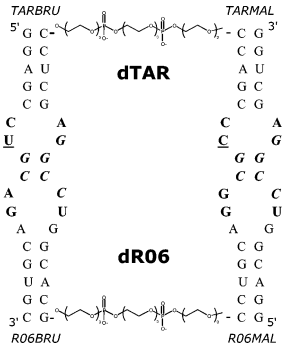

FIGURE 1: Sequence and secondary structure of the model system. The target, dTAR, consists of the TAR BRU hairpin linked to TAR MAL by three triethylene glycol phosphate units. BRU and MAL refer to two HIV-1 strains differing by one base in the apical loop (the mutated base is underlined). To generate the double ligand, dR06, the R06BRU hairpin was connected to R06MAL by the same linker used in dTAR. The loop bases that could potentially pair are shown with bold type. The three G's in the target loops or the three C's in the ligand ones that were substituted with three A's to generate the mutated dTAR or dR06 are in italics. MAL* or BRU* in the text will refer to a mutated MAL or BRU loop, respectively, either on the target or on the ligand side.

Second, a model that describes an interaction between one analyte and two independent ligands was used:

$$A_1 + B \underset{k_{off1}}{\overset{k_{on1}}{\rightleftharpoons}} A_1B$$

$$A_2 + B \underset{k_{off2}}{\overset{k_{on2}}{\rightleftharpoons}} A_2B$$

Then the sensorgrams obtained are simply the sum of the two independent reactions and can be fitted according to eqs 4 and 5 for the association and dissociation phases, respectively:

$$R = \frac{k_{on1}CR}{k_{on1}C + k_{off1}}1 - e^{-(k_{on1}C + k_{off1})(t - t_0)} + \frac{k_{on2}CR}{k_{on2}C + k_{off2}}1 - e^{-(k_{on2}C + k_{off2})(t - t_0)} \quad (4)$$

$$R = R_{t0}e^{-k_{off1}(t - t_0)} + R_{t0}e^{-k_{off2}(t - t_0)} \quad (5)$$

where R is the signal response, R_{max} the maximum response level, R_{t0} the response at the end of the injection, and C the molar concentration of the injected RNA molecule, k_{on} and k_{off} are the association and dissociation rate constants, respectively, and the numbers 1 and 2 refer to the two different sets of kinetic parameters.

RESULTS

Design of the Model System. To validate the use of bivalent RNA molecules as ligands for nonlinear RNA targets, a model was developed on the basis of a kissing complex identified by in vitro selection against TAR (*9*). Two HIV-1 variants of TAR, BRU and MAL, that differ mainly by a single mutation in the loop were used for generating a bifunctional target (Figure 1). Both individual hairpins were truncated above the bulge that constitutes part of the binding site for the viral protein Tat (*10*, *11*). A GC pair was added at the bottom of each stem to stabilize the hairpin structure.

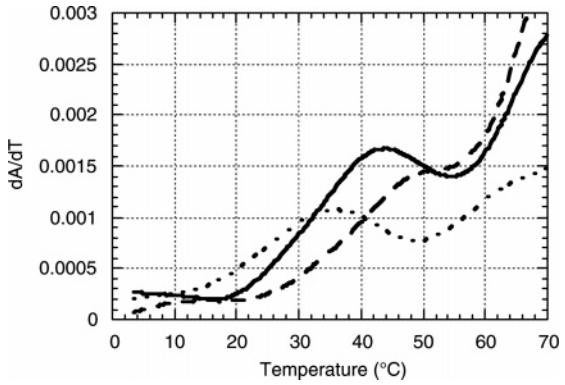

FIGURE 2: Interaction analysis of the double loop−loop complex model. First-derivative UV (260 nm) melting curves of dTAR complexed with R06BRU (···), with R06MAL (− − −), and with dR06 (—). The experiments were performed with each oligomer at 1 μM in 20 mM sodium cacodylate buffer (pH 7.3 and 20 °C) containing 140 mM potassium chloride, 20 mM sodium chloride, and 1 mM magnesium chloride.

Initially, TARBRU and TARMAL were connected by a 10-nucleotide linker equivalent in length to the one connecting the two hairpins of the *fhla* mRNA, a natural species giving rise to a bifunctional kissing complex. However, multiple migrating bands were observed on acrylamide gels, suggesting alternative foldings involving the linker. Three triethylene glycol phosphate units equivalent in length to the nucleotide linker were used to connect TARBRU and TARMAL truncated hairpins (Figure 1) to generate the bifunctional target, dTAR.

The bivalent ligand was derived from a shortened version of the 24-nucleotide RNA aptamer identified against the TAR BRU variant. The aptamer, R06BRU, derived from the parent one is 18 nucleotides long (Figure 1). It displays the same apical loop but has a shortened stem reduced to 5 bp, including the GC pair added at the bottom to stabilize the hairpin structure. The kissing aptamer selective for the TAR MAL variant, R06MAL, was derived from the R06BRU aptamer by introducing an A → G compensatory mutation into the aptamer loop as reported previously (*12*, *13*). R06BRU and R06MAL were connected by three triethylene glycol phosphate units to generate the bifunctional aptamer, dR06 (Figure 1).

Binding Properties of Single and Double Aptamers. Thermal denaturation experiments monitored by UV absorption spectroscopy were performed to compare the stability of single and double kissing complexes. The first derivatives of the thermal transitions characteristic of the bimolecular complexes are reported in Figure 2. The R06BRU−dTAR complex displays a melting temperature of 35.6 ± 0.2 °C (Table 1). The T_m for the R06MAL−dTAR complex is ∼50 °C but could not be determined precisely as this transition was close to that of the hairpins. Surprisingly, the dR06−dTAR complex displays a T_m of 43.8 ± 1.4 °C.

EMSA experiments were then performed to determine the apparent dissociation equilibrium constants. K_d values equal to 6.2 ± 2.0 and 1.0 ± 0.3 nM were obtained for the R06BRU−dTAR and R06MAL−dTAR complexes, respectively (Table 1). The dissociation equilibrium constant for the dR06−dTAR complex could not be determined by this method since at the lowest concentration that was used, 0.4

Table 1: Melting Temperatures (T_m) and Apparent Dissociation Constants (K_d) of the Complexes Formed between the Single Ligands, R06BRU and R06MAL, or the Double One, dR06, and dTAR or the Mutated Targets on the BRU Loop (dTARBRU*) and on the MAL Loop (dTARMAL*)

	T_m (°C)			K_d (nM)		
	dTAR	dTARMAL*	dTARBRU*	dTAR	dTARMAL*	dTARBRU*
R06BRU	35.6 ± 0.2	33.0 ± 0.7	nd[a]	6.2 ± 2.0	11.7 ± 0.1	>2000
R06MAL	~50	19.4 ± 0.6	~50	1.0 ± 0.3	>2000	3.9 ± 0.9
dR06	43.8 ± 1.4	34.5 ± 0.5	~50	<0.4	6.9 ± 2.8	1.2 ± 0.1

[a] Not determined.

Table 2: Rate Constants for Ligand−dTAR Complexes[a]

	k_{on1} ($\times 10^4$ M^{-1} s^{-1})	k_{off1} ($\times 10^{-4}$ s^{-1})	k_{on2} ($\times 10^3$ M^{-1} s^{-1})	k_{off2} ($\times 10^{-4}$ s^{-1})	K_{D1} (nM)	K_{D2} (nM)
R06BRU	4.97 ± 1.62	8.63 ± 0.56			17.4 ± 6.8	
dR06MAL*	1.90 ± 0.54	6.64 ± 0.04			34 ± 10	
R06MAL	0.43 ± 0.07	137 ± 10	3.93 ± 1.35	2.68 ± 0.84	3186 ± 751	68 ± 45
dR06BRU*	0.84 ± 0.22	117 ± 3	3.89 ± 1.80	1.49 ± 0.22	1196 ± 350	38 ± 24
dR06	3.92 ± 0.98	0.38 ± 0.11	8.67 ± 3.30	1.14 ± 0.36	0.97 ± 0.52	13 ± 9

[a] K_d was calculated as k_{off}/k_{on}, and the surface plasmon resonance experiments were performed at 23 °C in 20 mM HEPES (pH 7.3) containing 20 mM sodium acetate, 140 mM potassium acetate, and 1 mM magnesium acetate, as described in Materials and Methods.

nM, ~90% of the radiolabeled ligand was shifted (data not shown).

The model system was further investigated with monovalent or bivalent aptamers and mutated dTAR targets, either on the BRU loop (dTARBRU*) or on the MAL one (dTARMAL*). These TAR mutants were generated by substituting the three Gs in the loop with three As (Figure 1), given that these mutations drastically decreased the stability of the TAR−aptamer complexes as shown previously (*9*). Similar T_m's (~34 °C) and K_d's (~9 nM) were obtained for R06BRU−dTAR complexes whether the TAR MAL loop was mutated (Table 1). The interaction of R06BRU with dTARBRU* was no longer observed by either thermal denaturation experiments or EMSA. These results clearly indicate that R06BRU interacts specifically with its cognate hairpin.

No binding of R06MAL to dTARMAL* was detected by EMSA (K_d > 2000 nM), but a clear thermal transition was observed with a T_m of 19.4 °C indicating that the MAL aptamer recognized the TAR BRU hairpin in agreement with previous results (*12*, *13*).

Finally, the interaction between dR06 and the mutated dTAR targets was analyzed. The T_m's for dR06−dTARMAL* and dR06−dTARBRU* complexes are 34.5 ± 0.5 and ~50 °C, respectively (Table 1), suggesting single loop−loop interactions. The K_d values obtained for these complexes are consistent with those obtained for complexes between the single aptamers and the dTAR targets. Indeed, these results indicate that the two binding sites behave independently when the aptamers are not linked or when one site of the double target is mutated.

Kinetic Analysis of the Model System. SPR experiments were performed in an effort to understand the origin of the increased stability of the double kissing complex over the single ones. In such kinetic experiments, more than one complex can be detected and the corresponding binding rates determined.

The sensorgrams obtained when R06BRU or dR06MAL* analytes were injected on the sensor chip surface on which dTAR was immobilized are similar (data not shown). The rate constants could be determined assuming one reaction as previously shown with the parent RNA aptamer (*12*, *13*).

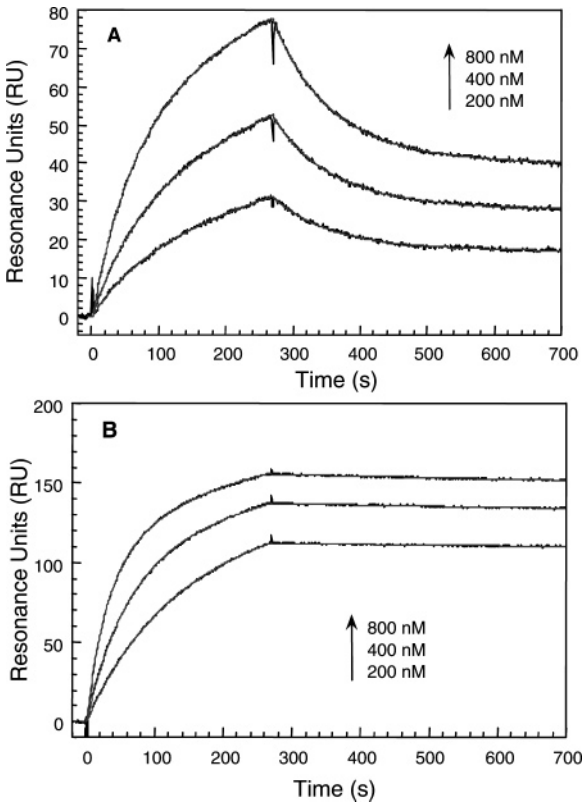

FIGURE 3: Sensorgrams of dTAR−dR06 complexes. Increasing concentrations of dR06BRU* (A) or dR06 (B) as indicated by the arrows were injected on the dTAR-functionalized CM5 sensor chip. The sensorgrams were fitted (gray lines) with a model that describes an interaction between one injected analyte and two independent immobilized sites. The elementary rate constants, k_{on} and k_{off}, were deduced from these fits according to eqs 4 and 5 (see Materials and Methods). Experiments were carried out at 23 °C in 20 mM HEPES buffer (pH 7.3), at 20 °C, containing 20 mM sodium acetate, 140 mM potassium acetate, and 1 mM magnesium acetate.

Both complexes display rate constants in the same range and are equivalent for binding to dTAR as shown by the K_d values deduced from the ratio k_{off}/k_{on} (Table 2).

Sensorgrams obtained for binding of R06MAL or dR06BRU* to dTAR are similar. Only those obtained for dR06BRU* are reported in Figure 3. These sensorgrams could only be fitted with two parallel reactions (see Materials

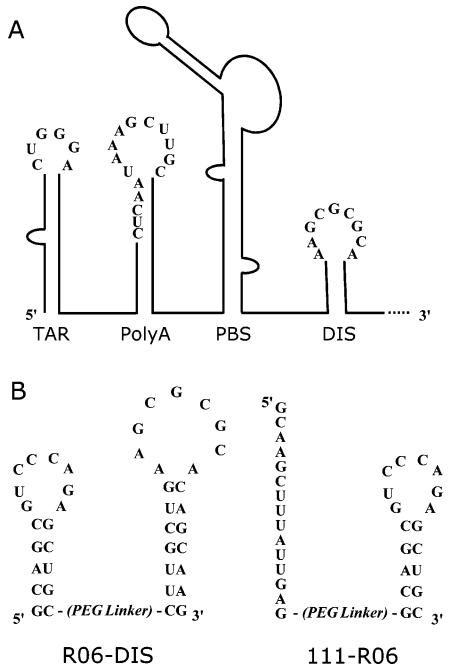

FIGURE 4: Secondary structure of the 5′UTR and design of the bivalent ligands. (A) Secondary structure of the 5′UTR showing the targeted hairpins. (B) Sequence and secondary structure of the ligands directed against TAR and DIS (left), and TAR and poly-(A) (right). Antisense 111, raised against the polyA hairpin, is complementary to the apical loop and part of the stem on the 5′ side. R06 is the hairpin aptamer that recognizes the TAR RNA of the HIV-1 BRU variant through loop−loop interactions. The DIS hairpin is the dimerization initiation site which self-associates and forms a loop−loop complex. PEG linker refers to two hexaethylene glycol phosphate units used to join the individual molecules.

and Methods). The rate constants and the calculated dissociation equilibrium constants for these reactions are listed in Table 2. These biphasic kinetics are consistent with the results that showed that the MAL aptamer also recognized the BRU target (*12*, *13*). Therefore, in light of these works, K_{D1} (∼2.2 μM) and K_{D2} (∼53 nM) can be ascribed to the MAL−BRU and MAL−MAL complexes, respectively.

The double hairpin aptamer, dR06, was then injected over the sensor chip surface. Compared to all other kinetics, the sensorgrams display very slow dissociation phases (Figure 3B). Only the parallel reaction model fitted the data, suggesting again that two reactions were followed. One reaction is characterized by rate constants, k_{on2} and k_{off2}, close to those obtained with R06MAL or dR06BRU* and therefore might reflect the formation of a MAL−MAL complex (Table 2). The other is characterized by a very slow dissociation rate of 3.8×10^{-5} s^{-1} and an on-rate of 3.9×10^{4} M^{-1} s^{-1} giving rise to the complex with the highest stability ($K_d \sim 1$ nM) that likely corresponds to the expected bivalent kissing complex.

Targeting the HIV-1 5′UTR with Bifunctional Ligands. The 5′ untranslated end of HIV-1 mRNAs folds as multiple hairpins (Figure 4A). Each of them playing a critical role in the regulation of the viral cycle (*14*) is potentially a valuable target for the design of ligands that could interact simultaneously with two hairpins. The dimerization initiation site (DIS) of HIV-1, for instance, has been shown to trigger the retroviral RNA dimerization (*15*−*19*) through the formation of a transient kissing complex between two DIS elements. This complex provides an interesting opportunity to test

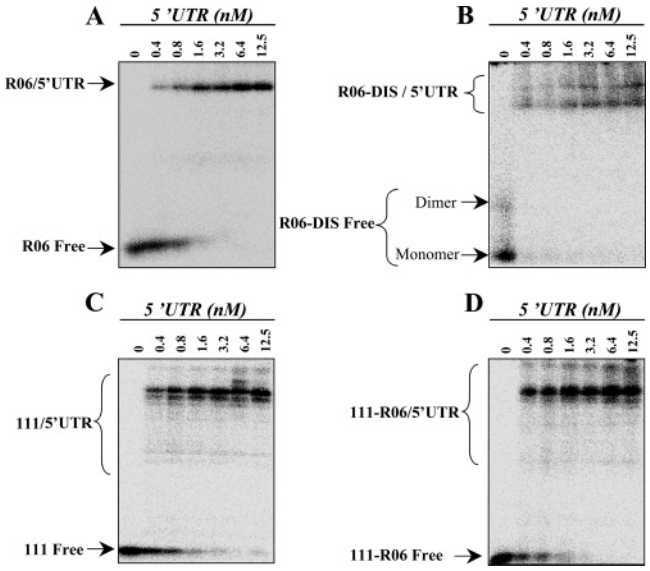

FIGURE 5: Analysis of ligand−5′UTR complexes by EMSAs. Radiolabeled R06 (A), R06-DIS (B), antisense 111 (C), or antisense 111-R06 (D) was incubated at 23 °C in 20 mM HEPES buffer (pH 7.3), at 20 °C, containing 20 mM sodium acetate, 140 mM potassium acetate, and 3 mM magnesium acetate with increasing amounts of 5′UTR as indicated above each lane (nanomolar). The arrows to the left indicate free radiolabeled ligands. The slowly migrating bands were used to determine the apparent binding constants (K_d) (see Materials and Methods).

whether a DIS haipin linked to R06BRU would generate a bivalent ligand of increased affinity for the 5′UTR compared to the individual ligands.

Radiolabeled R06BRU and increasing amounts of 5′UTR result in the appearance of a retarded band detected by an EMSA (Figure 5A). The apparent dissociation equilibrium constant, K_d, is 3.6 ± 1.1 nM. In contrast, no complex was detected with the DIS hairpin alone in the concentration range used for these experiments (data not shown). The apparent binding constant for the viral 5′UTR is >200 nM.

R06BRU and DIS hairpins were then connected to each other by two hexaethylene glycol phosphate units (Figure 4B). Two bands are observed in the absence of the 5′UTR (Figure 5B, lane 0), suggesting that R06BRU-DIS dimerizes. However, this reaction did not prevent binding to the target. Adding the double ligand to the 5′UTR led to two slowly migrating bands. To check whether these bands could reflect a dimerization reaction of the 5′UTR itself through its DIS motif, displacement of the radiolabeled 5′UTR with unlabeled 5′UTR was performed (data not shown). The results demonstrate that these bands rather correspond to two conformations of the viral target as no displacement was observed. These observations are consistent with a study that showed that the HIV-1 leader RNA might exist in vitro in two alternative conformations (*20*−*22*). These two bands are not observed with the individual R06BRU ligand (Figure 5A), suggesting that the two alternative conformations originate in the interaction with the bivalent R06BRU-DIS ligand. The apparent dissociation equilibrium constant could not be determined as at the lowest concentration that was used, 0.4 nM, the radiolabeled ligand was totally shifted (Figure 5B).

To investigate further the use of bimodal interactions in generating ligands of increased affinity for structured RNA targets, two adjacent hairpins, TAR and poly(A) (Figure 4A), were targeted. Using R06BRU as one of the partners, the

design of the bifunctional ligand required the identification of an oligomer that could interact with the poly(A) hairpin. The rational design of a structured ligand interacting with poly(A) through loop−loop interactions would have been hazardous. This approach, used for instance to identify a ligand that would form a kissing complex with TAR (*23*, *24*), led to a much poorer ligand than the hairpin aptamer identified by in vitro selection (*25*). Even if the interaction is driven primarily by the loop complementarity, noncanonical interactions such as base stacking at the stem−loop junctions and interbackbone hydrogen bonds were shown to be critical for the stability of loop−loop complexes (*26*−*28*). On a rational basis, these types of interaction are difficult to predict, not to say impossible. Rather than selecting an aptamer to the poly(A) hairpin, we took advantage of the size of the apical loop of this element. This allowed us to design a sufficiently long antisense oligonucleotide that minimally unfolds the upper stem.

Antisense oligonucleotides 11 to 15-nucleotide RNA were designed to bind to various regions of the apical part of the poly(A) stem−loop structure. Oligomer 111, 5′-GCAAGCUUUAUUGAG-3′, complementary to the 5′ side of the stem and part of the loop (Figure 4A), was chosen for these experiments as it displayed an affinity for its target in the low nanomolar range (data not shown). Formation of the complex between antisense 111 and the 5′UTR results in the appearance of multiple slowly migrating bands (Figure 5C), suggesting that several complexes are formed. The two major bands could be ascribed to the binding of antisense 111 to the two conformations of the 5′UTR. The minor bands that represent no more than 10% in the total radioactivity of each lane likely reflect nonspecific binding of the antisense oligonucleotide to the target. The two major retarded bands were used to determine an apparent K_d (1.5 ± 0.1 nM) for the antisense 111−5′UTR complex.

Antisense 111 and R06BRU were then connected by two hexaethylene glycol phosphate units (Figure 4B), and the affinity of this ligand for the 5′UTR was determined by EMSA. Multiple bands are also observed, which, in light of the results obtained with antisense 111 alone (Figure 5C), can be attributed to nonspecific binding of the antisense part of the double ligand. The apparent K_d deduced from the analysis of the two major retarded bands is 0.8 ± 0.2 nM.

DISCUSSION

A model of interaction that aimed at demonstrating that bimodal RNA−RNA interactions can generate higher-stability complexes in a structured context was investigated. This model consisted of a double kissing complex formed between two TAR variants, BRU and MAL, connected by a non-nucleotidic linker on one hand and the corresponding R06 aptamer hairpins connected by the same linker on the other hand (Figure 1). This bimodal interaction provided an enhanced stability for the double kissing complex compared to the individual ones that resulted from a slower dissociation rate.

The chemical linker was chosen to prevent alternative conformations of the designed hairpins, and its length provided a connection equivalent to ∼10 nucleotides. The question of whether this link is optimized with regard to its length and composition arises. It is probably not optimized, as the advantage provided by the bimodal interaction is smaller than the theoretical advantage. We choose arbitrarily to connect the R06BRU aptamer and the DIS hairpin with two hexaethylene glycol phosphate units. Connectors of length from zero to three were also tested, but the apparent equilibrium constant determined by EMSA experiments remained unchanged (K_d < 0.4 nM). This could be further investigated.

The T_m measured for the double kissing complex (43.8 °C) is unexpected. It lies between the one obtained for the R06BRU−dTAR complex (35.6 °C) and the one for the R06MAL−dTAR complex (∼50 °C). To investigate whether the bimodal interaction could result in a shift of the two individual loop−loop interactions such that the second transition was hidden under the transition for unfolding the hairpins, thermal denaturation experiments were performed at lower magnesium concentrations. The stability of kissing complexes is well-known to depend on magnesium ion, while the stability of the hairpin stems remains nearly unchanged (*25*, *26*). Decreasing the magnesium concentration from 1 to 0.1 mM resulted in the appearance of a single thermal transition with a T_m of 28 °C, and no second transition was observed between this transition and the one reflecting the unfolding of the hairpins (data not shown). When single R06BRU and R06MAL aptamers were mixed together and allowed to interact simultaneously with dTAR, at 1 mM magnesium, two thermal transitions that matched exactly those obtained for the R06BRU−dTAR and R06MAL−dTAR complexes were observed (data not shown), indicating that such a ternary complex behaved as two independent kissing complexes. In addition, the double kissing complex migrated faster on a native polyacrylamide gel when the two aptamers were connected than when they were allowed to interact together as single hairpins (data not shown). This definitively demonstrates that the double kissing complex adopts a new conformation that might explain why a single thermal transition is observed, reflecting the simultaneous melting of the two kissing complexes. This conformation is recognized by Rop (data not shown), a protein which binds specifically loop−loop helices, further emphasizing that the double aptamer and target are engaged in loop−loop interactions.

TAR and poly(A) hairpins were targeted with a ligand consisting of the R06BRU aptamer connected to an antisense oligonucleotide complementary to part of the apical poly(A) stem−loop structure. The resulting bifunctional complex displayed a slight increase in stability compared to those formed with the individual ligands. In addition, multiple bands were observed that indicated the formation of several complexes, raising the question about the specificity of the interaction. In contrast, a unique retarded band was detected when antisense 111 was allowed to interact with the truncated poly(A) hairpin (data not shown). This underlines one of the limitations of the antisense strategy when larger targets are used. No such behavior was observed with aptamers. We recently showed that hairpin aptamers more specifically discriminate between wild-type and point-mutated targets than antisense oligonucleotides with similar affinity (F. Darfeuille et al., unpublished observations). These results suggest that in a context where multiple species interact simultaneously, structured RNA aptamers would provide better tuning of the interaction with nonlinear RNA targets

as recognition is achieved also on the basis of the three-dimensional structure.

Beyond our own work, bivalent ligands were previously assayed against RNA. Tethered oligonucleotide probes (TOPs) consisting of two short oligonucleotides joined by a chemical tether were developed to target the HIV Rev response element (RRE). These ligands, however, were designed to recognize two accessible single-stranded sequences within the folded RNA (*29*, *30*). Triplex TOPs that interact simultaneously with one single-stranded region and one double-stranded region of the RRE through the formation of Watson−Crick and Hoogsteen base pairs, respectively, were also generated (*31*). All complexes formed with these bivalent oligonucleotides displayed enhanced stability compared to those formed with the individual oligonucleotides. An entropically favorable second binding was also used to induce the cleavage of a hardly inaccessible site within a messenger RNA by a "maxizyme" that was composed of two substrate-binding arms. This "double" ribozyme not only was more efficient than a monovaent one but also could bind and cleave a stem structure that was supposed to be inaccessible to a ribozyme (*32*, *33*).

In conclusion, our work demonstrates that bifunctional aptamers might provide a way of targeting structured RNA targets with no need to unfold them. In addition to the enhanced stability of the resulting complexes that can be expected from multiple simultaneous interactions, specificity could be improved as recognition is also achieved on the basis of the three-dimensional structure.

ACKNOWLEDGMENT

We thank Dr. Ben Berkhout for the generous gift of the Bluescript-5′LTR plasmid and Nathalie Pierre for the RNA molecules synthesized on the Expedite 8908 synthesizer.

REFERENCES

1. Brunel, C., Marquet, R., Romby, P., and Ehresmann, C. (2002) RNA loop-loop interactions as dynamic functional motifs, *Biochimie 84*, 925−44.
2. Tomizawa, J. (1986) Control of ColE1 plasmid replication: Binding of RNA I to RNA II and inhibition of primer formation, *Cell 47*, 89−97.
3. Tomizawa, J. (1990) Control of ColE1 plasmid replication. Intermediates in the binding of RNA I and RNA II, *J. Mol. Biol. 212*, 683−94.
4. Wagner, E. G., and Simons, R. W. (1994) Antisense RNA control in bacteria, phages, and plasmids, *Annu. Rev. Microbiol. 48*, 713−42.
5. Wassarman, K. M., Zhang, A., and Storz, G. (1999) Small RNAs in *Escherichia coli*, *Trends Microbiol. 7*, 37−45.
6. Altuvia, S., Zhang, A., Argaman, L., Tiwari, A., and Storz, G. (1998) The *Escherichia coli* OxyS regulatory RNA represses fhlA translation by blocking ribosome binding, *EMBO J. 17*, 6069−75.
7. Altuvia, S., and Wagner, E. G. (2000) Switching on and off with RNA, *Proc. Natl. Acad. Sci. U.S.A. 97*, 9824−6.
8. Argaman, L., and Altuvia, S. (2000) fhlA repression by OxyS RNA: Kissing complex formation at two sites results in a stable antisense-target RNA complex, *J. Mol. Biol. 300*, 1101−12.
9. Ducongé, F., and Toulmé, J. J. (1999) In vitro selection identifies key determinants for loop-loop interactions: RNA aptamers selective for the TAR RNA element of HIV-1, *RNA 5*, 1605−14.
10. Karn, J. (1999) Tackling Tat, *J. Mol. Biol. 293*, 235−54.
11. Richter, S., Ping, Y. H., and Rana, T. M. (2002) TAR RNA loop: A scaffold for the assembly of a regulatory switch in HIV replication, *Proc. Natl. Acad. Sci. U.S.A. 99*, 7928−33.
12. Darfeuille, F., Arzumanov, A., Gryaznov, S., Gait, M. J., Di Primo, C., and Toulmé, J. J. (2002) Loop-loop interaction of HIV-1 TAR RNA with N3′→P5′ deoxyphosphoramidate aptamers inhibits in vitro Tat-mediated transcription, *Proc. Natl. Acad. Sci. U.S.A. 99*, 9709−14.
13. Darfeuille, F., Arzumanov, A., Gait, M. J., Di Primo, C., and Toulmé, J. J. (2002) 2′-O-Methyl-RNA Hairpins Generate Loop-Loop Complexes and Selectively Inhibit HIV-1 Tat-Mediated Transcription, *Biochemistry 41*, 12186−92.
14. Berkhout, B. (2000) Multiple biological roles associated with the repeat (R) region of the HIV-1 RNA genome, *Adv. Pharmacol. 48*, 29−73.
15. Skripkin, E., Paillart, J. C., Marquet, R., Ehresmann, B., and Ehresmann, C. (1994) Identification of the primary site of the human immunodeficiency virus type 1 RNA dimerization in vitro, *Proc. Natl. Acad. Sci. U.S.A. 91*, 4945−9.
16. Paillart, J. C., Skripkin, E., Ehresmann, B., Ehresmann, C., and Marquet, R. (1996) A loop-loop "kissing" complex is the essential part of the dimer linkage of genomic HIV-1 RNA, *Proc. Natl. Acad. Sci. U.S.A. 93*, 5572−7.
17. Muriaux, D., Fosse, P., and Paoletti, J. (1996) A kissing complex together with a stable dimer is involved in the HIV-1Lai RNA dimerization process in vitro, *Biochemistry 35*, 5075−82.
18. Jossinet, F., Paillart, J. C., Westhof, E., Hermann, T., Skripkin, E., Lodmell, J. S., Ehresmann, C., Ehresmann, B., and Marquet, R. (1999) Dimerization of HIV-1 genomic RNA of subtypes A and B: RNA loop structure and magnesium binding, *RNA 5*, 1222−34.
19. Ennifar, E., Walter, P., Ehresmann, B., Ehresmann, C., and Dumas, P. (2001) Crystal structures of coaxially stacked kissing complexes of the HIV-1 RNA dimerization initiation site, *Nat. Struct. Biol. 8*, 1064−8.
20. Huthoff, H., and Berkhout, B. (2001) Two alternating structures of the HIV-1 leader RNA, *RNA 7*, 143−57.
21. Berkhout, B., Ooms, M., Beerens, N., Huthoff, H., Southern, E., and Verhoef, K. (2002) In vitro evidence that the untranslated leader of the HIV-1 genome is an RNA checkpoint that regulates multiple functions through conformational changes, *J. Biol. Chem. 277*, 19967−75.
22. Ooms, M., Verhoef, K., Southern, E., Huthoff, H., and Berkhout, B. (2004) Probing alternative foldings of the HIV-1 leader RNA by antisense oligonucleotide scanning arrays, *Nucleic Acids Res. 32*, 819−27.
23. Chang, K. Y., and Tinoco, I., Jr. (1994) Characterization of a "kissing" hairpin complex derived from the human immunodeficiency virus genome, *Proc. Natl. Acad. Sci. U.S.A. 91*, 8705−9.
24. Chang, K. Y., and Tinoco, I., Jr. (1997) The structure of an RNA "kissing" hairpin complex of the HIV TAR hairpin loop and its complement, *J. Mol. Biol. 269*, 52−66.
25. Ducongé, F., Di Primo, C., and Toulmé, J. J. (2000) Is a closing "GA pair" a rule for stable loop-loop RNA complexes? *J. Biol. Chem. 275*, 21287−94.
26. Gregorian, R. S., Jr., and Crothers, D. M. (1995) Determinants of RNA hairpin loop-loop complex stability, *J. Mol. Biol. 248*, 968−84.
27. Kim, C. H., and Tinoco, I., Jr. (2000) A retroviral RNA kissing complex containing only two G·C base pairs, *Proc. Natl. Acad. Sci. U.S.A. 97*, 9396−401.
28. Beaurain, F., Di Primo, C., Toulmé, J. J., and Laguerre, M. (2003) Molecular dynamics reveals the stabilizing role of loop closing residues in kissing interactions: Comparison between TAR-TAR* and TAR-aptamer, *Nucleic Acids Res. 31*, 4275−84.
29. Cload, S. T., and Schepartz, A. (1991) Polyether tethered oligonucleotide probes, *J. Am. Chem. Soc. 113*, 6324−6.
30. Cload, S. T., and Schepartz, A. (1994) Selection of structure-specific inhibitors of the HIV Rev-Rev response element complex, *J. Am. Chem. Soc. 116*, 437−42.
31. Moses, A. C., and Schepartz, A. (1997) Kinetics and mechanism of RNA binding by triplex tethered oligonucleotide probes, *J. Am. Chem. Soc. 119*, 11591−7.
32. Kuwabara, T., Warashina, M., Tanabe, T., Tani, K., Asano, S., and Taira, K. (1998) A novel allosterically trans-activated ribozyme, the maxizyme, with exceptional specificity in vitro and in vivo, *Mol. Cell 2*, 617−27.
33. Kuwabara, T., Warashina, M., and Taira, K. (2002) Cleavage of an inaccessible site by the maxizyme with two independent binding arms: An alternative approach to the recruitment of RNA helicases, *J. Biochem. 132*, 149−55.

BI051187F